1 March 2001

ELSEVIER

Optics Communications 189 (2001) 135–142

OPTICS COMMUNICATIONS

www.elsevier.com/locate/optcom

Efficient nonlinear infrared parametric generation in one-dimensional photonic band gap structures

M. Centini [a,b], M. Scalora [b,c,*], G. D'Aguanno [a,b], C. Sibilia [a], M. Bertolotti [a], M.J. Bloemer [b], C.M. Bowden [b], J.W. Haus [d]

[a] *INFM at Dipartimento di Energetica, Università di Roma "La Sapienza", Via Scarpa 16, 00161 Rome, Italy*
[b] *US Army Aviation and Missile Command, Weapon Sciences Directorate, AMSMI-RD-WS-ST Redstone Arsenal, Huntsville, AL 35898-5000, USA*
[c] *Time Domain Corporation, Cummings Research Park, 7057 Old Madison Pike, Huntsville, AL 35806-6400, USA*
[d] *Electro-Optics Program, University of Dayton, Dayton OH 45469-0245, USA*

Received 22 September 2000; accepted 11 December 2000

Abstract

Using numerical methods and the effective index approach that we recently discussed in a separate publication, we show that it is possible to obtain highly efficient, phase matched nonlinear generation of infrared (3 μm) radiation in a one-dimensional photonic band gap structure. We predict conversion efficiencies that approach pump depletion in single-pass geometry, assuming $\chi^{(2)}$ values of order 100 pm/V, and pump intensities of order 100 MW/cm^2. © 2001 Published by Elsevier Science B.V.

Keywords: Photonic bad gap; Nonlinear frequency conversion; Downconversion; Infrared; Parametric

1. Introduction

Photonic band gap (PBG) materials have enjoyed a great deal of attention because devices based on the physics of photonic band edge appear to posses the potential for significant technological advances [1–11]. While most studies are directed toward the realization of three-dimensional PBGs, in which a gap appears in all possible directions of incidence, it may be preferable to first study one-dimensional (1-D) multilayer stacks because of their simplicity. Therefore, we focus our attention on 1-D structures.

The study of nonlinear optical interactions in 1-D PBG structures has been undertaken mainly in regard to soliton-like pulses (often referred to as gap solitons) in cubic $\chi^{(3)}$ [12–16] and quadratic $\chi^{(2)}$ media [17]. Second harmonic generation (SHG) has recently been experimentally observed under different circumstances. As an example, we cite the experimental observation of SHG in a centrosymmetric crystalline lattice of dielectric spheres [18–20], in a semiconductor microcavity [21], near the band edge of a ZnS/SrF multilayer stack [22], where an order of magnitude enhancement of SH intensity over bulk material was

* Corresponding author. Address: Time Domain Corporation, Cummings Research Park, 7057 Old Madison Pike, Huntsville, AL 35806-6400, USA. Fax: +1-256-955-7216.
E-mail address: mscalora@ws.redstone.army.mil (M. Scalora).

0030-4018/01/$ - see front matter © 2001 Published by Elsevier Science B.V.
PII: S0030-4018(01)00994-4

reported. This communication adds to our previous work on the dynamics of ultrashort pulses propagating in finite, $\chi^{(2)}$ active, PBG structures [9,10,23,24]. Earlier, we predicted that near the photonic band edge of a 1-D PBG structure SHG could be enhanced by several orders of magnitude [9,10]. We showed that there were several reasons for such large enhancement: first, an increase in the density of modes takes place near the band edge; second, strong mode overlap occurs; third, small group velocities insure increased interaction times. Later, we developed an effective index approach for finite structures that allowed us to examine the phase properties of the interacting fields, and showed that the conditions outlined above are also accompanied, remarkably, by the possibility to realize exact phase-matching conditions [23]. That is, while it is important to have high mode density, field overlap, and large interaction times, global, effective phase-matching conditions play an equally important role in the final determination of conversion efficiency [23].

In this paper, we extend the analysis we began with the introduction of an effective dispersion relation for the finite structure by examining in some detail another important aspect of nonlinear frequency conversion, that is down-conversion processes. Using the effective index approach, we first derive simple phase-matching conditions for three-wave coupling, and then test them by numerically integrating the equations of motion in the time domain. We specifically set out to explore the possibility of generating near and far infrared radiation through a three-wave mixing process in micron-sized PBG structures because there is a conspicuous absence in the market place of small volume, reliable, coherent sources of radiation in that range. The amplification of sum-frequency generation was recently reported [25] for pumps that were tuned near the band edge of a 1-D structure. In Ref. [25] the authors show that the increase in the density of modes near the band edge can lead to the generation of 400 nm radiation at a rate that was approximately one order of magnitude higher compared to the case where the pumps where not tuned near the band edge. However, no particular care was exercised in that case to make sure that phase-matching conditions that we describe in Ref. [23] were satisfied. Therefore, we predict that if the scheme we propose for phase matching is implemented in a 1-D geometry, enhancements will be much larger.

The typical 1-D structure that we consider consists of alternating layers of high and low index materials. We assume that two pump fields, for example, at ω_1 ($\lambda = 3$ μm) and ω_2 ($\lambda = 1.5$ μm), are incident normally on the structure, and that their interaction, mediated by a $\chi^{(2)}$ process, generates a down-converted signal at a third frequency ω_3 ($\lambda = 1$ μm). So initially there is no ω_1 signal. The specific wavelengths that we use here are not crucial, and are used for illustration purposes only. It will become clear later, as we also showed previously [23], that both material and geometrical dispersion can be combined to produce exact phase-matching conditions for a variety of situations, a fact that highlight the flexibility of these devices.

The approach that we pursue is as follows: first, we design a multilayer stack, and determine its linear phase properties using the effective index formulation. We seek appropriate tuning of all the fields with respect to their respective band edges in order to simultaneously optimize and combine phase-matching conditions with high density of modes [23]. Then, we integrate the nonlinear, coupled equations of motion in the time domain. For clarity and completeness, we briefly outline both the effective index approach and the integration method that we use, which were discussed in detail elsewhere.

2. Effective index method

We now review a method based on a formulation of the effective dispersion relation that allows us to evaluate the effective refractive index for a multilayered structure. Using the matrix transfer method [23,26], we define a general transmission function for any structure as follows:

$$t \equiv x + \mathrm{i}y \equiv \sqrt{T}\mathrm{e}^{\mathrm{i}\varphi_\mathrm{t}}, \tag{1}$$

where $\sqrt{T}$ is the transmission amplitude, $\varphi_\mathrm{t} = \tan^{-1}(y/x) \pm m\pi$ is the total phase accumulated as light traverses the medium, and m is an integer

number. In analogy with the propagation in a homogeneous medium, we can express the total phase associated with the transmitted field as

$$\varphi_t = k(\omega)D = (\omega/c)n_{\text{eff}}(\omega)D, \tag{2}$$

where $k(\omega)$ is the effective wave vector; and n_{eff} is the effective refractive index that we attribute to the layered structure whose physical length is D. As described in Ref. [23], we obtain the following expression of the effective index of refraction:

$$\hat{n}_{\text{eff}} = (c/\omega D)[\varphi_t - (i/2)\ln(x^2 + y^2)]. \tag{3}$$

Eq. (3) suggests that at resonance, where $T = x^2 + y^2 = 1$, the imaginary part of the index is identically zero. We can also define the effective index as the ratio between the speed of light in vacuum and the effective phase velocity of the wave in the medium. We have

$$\hat{k}(\omega) = \frac{\omega}{c}\hat{n}_{\text{eff}}(\omega). \tag{4}$$

This is the effective dispersion relation of the finite structure. For periodic structures, the phase-matching conditions are automatically fulfilled if the fields are tuned at the right resonance peaks of the transmission spectrum. Using the formalism introduced in Ref. [27], the expression for the effective index for the N-periods finite structure can be recast as follow [23]:

$$\hat{n}_{\text{eff}} = \frac{c}{\omega N a}\left\{\tan^{-1}[z\tan(N\beta)\cot(\beta)] + \text{Int}\left[\frac{N\beta}{\pi} + \frac{1}{2}\right]\pi\right\}, \tag{5}$$

where β is the Bloch's phase for an infinite structure having the same identical unit cell as the finite structure in question. Eq. (5) contains additional information regarding the location of the resonances where phase matching for a three-wave mixing (TWM) process can occur. For illustration purposes, we consider a 20-period, mixed *half-wave/eight-wave* periodic structure. We choose this arrangement because it allows us to easily tune all the fields near their respective band edges, and thus allowing us to simultaneously access a high density of modes for all fields. We note that this arrangement is not unique, in that higher or lower order band edges can be combined to yield the phase-matching conditions, within the context of the effective index approach outlined in Ref. [23]. As before, we assume that two pump fields are tuned at $\omega_3 = 3\omega$, and $\omega_2 = 2\omega$; the interaction via a $\chi^{(2)}$ process then generates a down-converted signal at a third frequency $\omega_1 = \omega$ ($\lambda = 3$ μm). First, we tune the still-absent field of frequency ω_1 at the first resonance near the first-order band edge; this insures a high density of modes. We have [23]:

$$\beta_1 = \frac{\pi}{N}(N - 1). \tag{6}$$

Then, we tune the field ω_2 at the first resonance near the second-order band edge, once again securing a high density of modes; we have:

$$\beta_2 = \frac{\pi}{N}(2N - 1). \tag{7}$$

We now impose the phase-matching condition for the TWM process, namely:

$$K_3(\omega_3) - K_2(\omega_2) - K_1(\omega_1) = 0. \tag{8}$$

Substituting Eqs. (6) and (7) into Eq. (5), we obtain

$$\beta_3 = \frac{\pi}{N}(3N - 2) \tag{9}$$

which is the value of the Bloch's phase that will correspond to the field at frequency ω_3. This means that phase-matching conditions will be satisfied for this structure if the thickness of the layers (i.e. geometrical dispersion) are combined with material dispersion such that the first pump field is tuned to the second resonance away from the low frequency band edge of the third order gap $(3N - 2)$. The second pump and the generated fields are then tuned to the first resonance near their respective band edges. In Fig. 1 we depict the transmission spectrum of the structure we are considering, and also point out the relative tuning of all the fields. The caption contains the structure's data. We emphasize that in order to be able to tune the fields as specified we have used both the natural dispersion of the material and the geometrical dispersion of the structure. Thus, the dispersion induced by the geometry of the structure, in particular layer thicknesses, can be used to compensate the natural dispersion of material as shown in Fig. 1.

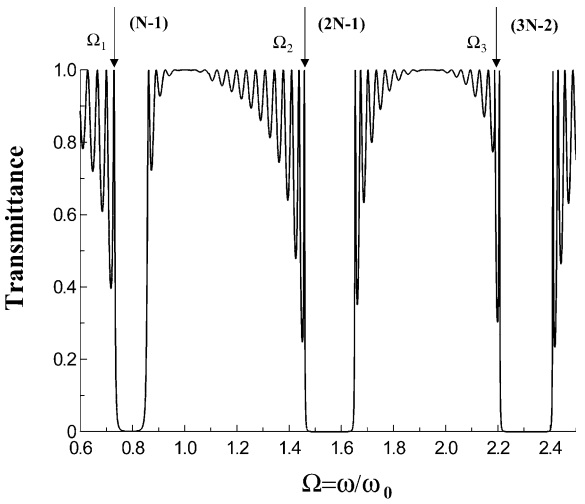

Fig. 1. Transmittance vs normalized frequency for a 20-period mixed half-wave/eight-wave structure. We use $n_1 = 1$ for the low index material at all frequencies. We have introduced a small amount of dispersion, typical of semiconductors, for example, such that: $n_2(\Omega_3) = 1.502$, $n_2(\Omega_2) = 1.475$, and $n_2(\Omega_1) = 1.4285714$. The fields are tuned near their respective band edges as follows: Ω_1 at the $(N-1)$th resonance, Ω_2 at the $(2N-1)$th resonance, and Ω_3 is tuned to the $(3N-2)$th resonance, to satisfy exact phase-matching conditions for the three-wave mixing process.

3. Equations of motion and pulse propagation formalism

The crystal is composed of 40 dielectric layers and the index of refraction alternates between a high and a low value. We assume normal dispersion, with $n_2(\omega) = 1.4285$, $n_2(2\omega) = 1.475$, $n_2(3\omega) = 1.502$, and $n_1 = 1$ (air) at all frequencies. We assume we are operating in a region where losses can be neglected, and the nonlinear material is distributed in the high index layers only, with $\chi^{(2)} \approx 100$ pm/V. We note that this particular choice of active layer location is not crucial, and has been chosen to correspond with the high index layer because at the low frequency band edges the fields localize in the high index layers. Therefore, one might envision a scheme for tuning the pumps at the high frequency band edge, which would require relocation of the nonlinear material to those layers. From a computational point of view, this choice is unimportant.

For a reference wavelength λ_0, corresponding to a frequency ω_0, the layers have thicknesses $a = \lambda_0/(8n_1)$ and $b = \lambda_0/(2n_2)$, respectively. A range of frequencies is reflected, as shown in Fig. 1, where we plot the transmittance as a function of the scaled frequency $\Omega = \omega/\omega_0$, where $\omega_0 = 2\pi c/\lambda_0$. The equations of motion can be derived beginning with Maxwell's equation for the total field, in Gaussian units, and can be written as:

$$\frac{\partial^2 E(z,t)}{\partial z^2} - \frac{n^2(z)}{c^2}\frac{\partial^2 E(z,t)}{\partial t^2} = \frac{4\pi}{c^2}\frac{\partial^2 P_{\mathrm{NL}}(z,t)}{\partial t^2}. \tag{10}$$

Here, P_{NL} is the total nonlinear polarization. The fields can arbitrarily and conveniently be decomposed as follows:

$$E(z,t) = \sum_1^3 \varepsilon_j(z,t)\mathrm{e}^{\mathrm{i}(k_j z - \omega_j t)} + \mathrm{c.c.} \tag{11}$$

and

$$P_{\mathrm{NL}}(z,t) = \sum_1^3 P_j(z,t)\mathrm{e}^{\mathrm{i}(k_j z - \omega_j t)} + \mathrm{c.c.} \tag{12}$$

$\varepsilon_j(z,t)$ and $P_j(z,t)$ are complex envelopes that take into account all linear and nonlinear phase modulation effects due to propagation. This decomposition of the fields is convenient because it allows us to extract the fields' vacuum wave vectors without loss of generality. Then we assume that $\omega_1 = \omega$, $\omega_2 = 2\omega$, and $\omega_3 = \omega_2 + \omega_1$ with $k_1 \equiv k = \omega/c$, $k_2 = 2\omega/c$, and $k_3 = 3\omega/c$. This choice of wave vectors corresponds to an initial condition consistent with pump fields initially propagating in free space, located away from the structure. Thus, our integrations closely simulate experimental conditions. We emphasize that any phase modulation effects that ensue from propagation, i.e., multiple reflections and nonlinear interactions, are fully accounted for in the dynamics of the field envelopes, which maintain their general complex form. It can then be shown that the nonlinear polarization takes the following form:

$$\begin{aligned} P_{\mathrm{NL}}(z,t) = \chi^{(2)}E^2(z,t) &= 2\chi^{(2)}\{\varepsilon_1^*\varepsilon_2 + \varepsilon_2^*\varepsilon_3\}\mathrm{e}^{\mathrm{i}(kz-\omega t)} \\ &+ 2\chi^{(2)}\{\varepsilon_1^*\varepsilon_3 + \tfrac{1}{2}\varepsilon_1^2\}\mathrm{e}^{\mathrm{i}(2kz-2\omega t)} \\ &+ 2\chi^{(2)}\varepsilon_1\varepsilon_2\mathrm{e}^{\mathrm{i}(3kz-3\omega t)} + \mathrm{c.c.}, \end{aligned} \tag{13}$$

where ε_1, ε_2 and ε_3 are the fields at the frequencies ω_1, ω_2, ω_3 respectively. While we can assume initial left- or right-propagating pump pulses (2ω and 3ω), the generated signal at frequency ω is initially zero everywhere. The direction of propagation of the spontaneously generated field, and the exact nature of the quasi-standing wave inside the structure depend from exact pump tuning and the structure parameters, and it is determined in a dynamic fashion. We are also considering propagation in the presence of large index discontinuities, and so we retain all second-order spatial derivatives. However, we assume that pulse envelopes have a duration that is always much greater than the optical cycle, thus allowing the application of the slowly varying envelope approximation in time (SVEAT) only [4–9,28]. The equations of motion for the fields can then be derived by substituting Eqs. (11)–(13) into Eq. (10), and by applying the SVEAT. The inclusion of all second-order spatial derivatives in the equations of motion means that reflections are accounted for to all orders, without any approximations. Details on the propagation method can be found in Refs. [4–9,28]. Therefore, assuming that pulses never become so short as to violate SVEAT (usually this means a few tens of optical cycles, if propagation distances are on the order of pulse width, as in our case. Neglect of the second-order temporal derivative usually means that if the pulse is too short and it is allowed to propagate over long distances, it begins to diffract), neglecting all but the lowest order temporal contributions to the dynamics, and using the nonlinear polarization expansions of Eq. (13), we have:

$$n_{2\Omega}^2(\xi)\frac{\partial}{\partial\tau}\varepsilon_{2\Omega}(\xi,\tau) = \frac{\mathrm{i}}{4\pi 2\Omega}\frac{\partial^2}{\partial\xi^2}\varepsilon_{2\Omega}(\xi,\tau) - \frac{\partial}{\partial\xi}\varepsilon_{2\Omega}(\xi,\tau) + \mathrm{i}\pi[n_{2\Omega}^2(\xi)-1]2\Omega\varepsilon_{2\Omega}(\xi,\tau) + \mathrm{i}8\pi^2 2\Omega\chi^{(2)}\{\varepsilon_{3\Omega}\varepsilon_{\Omega}^* + \tfrac{1}{2}\varepsilon_{\Omega}^2\}, \tag{14a}$$

$$n_{3\Omega}^2(\xi)\frac{\partial}{\partial\tau}\varepsilon_{3\Omega}(\xi,\tau) = \frac{\mathrm{i}}{4\pi 3\Omega}\frac{\partial^2}{\partial\xi^2}\varepsilon_{3\Omega}(\xi,\tau) - \frac{\partial}{\partial\xi}\varepsilon_{3\Omega}(\xi,\tau) + \mathrm{i}\pi[n_{3\Omega}^2(\xi)-1]3\Omega\varepsilon_{3\Omega}(\xi,\tau) + \mathrm{i}8\pi^2 3\Omega\chi^{(2)}\varepsilon_{2\Omega}\varepsilon_{\Omega}, \tag{14b}$$

$$n_{\Omega}^2(\xi)\frac{\partial}{\partial\tau}\varepsilon_{\Omega}(\xi,\tau) = \frac{\mathrm{i}}{4\pi\Omega}\frac{\partial^2}{\partial\xi^2}\varepsilon_{\Omega}(\xi,\tau) - \frac{\partial}{\partial\xi}\varepsilon_{\Omega}(\xi,\tau) + \mathrm{i}\pi[n_{\Omega}^2(\xi)-1]\Omega\varepsilon_{\Omega}(\xi,\tau) + \mathrm{i}8\pi^2\Omega\chi^{(2)}\{\varepsilon_{2\Omega}^*\varepsilon_{3\Omega} + \varepsilon_{2\Omega}\varepsilon_{\Omega}^*\}. \tag{14c}$$

From Eqs. (13) and (14) it is apparent that since we are considering harmonics of a fundamental field, there will be multiple contributions to the nonlinear source terms that might otherwise be ignored in the usual rotating wave approximation. In Eqs. (14), $\Omega = \omega/\omega_0$, $\xi = z/\lambda_0$, and $\tau = ct/\lambda_0$. The spatial coordinate z has been conveniently scaled in units of λ_0; the time is also conveniently expressed in units of the corresponding optical period. As we will see below, forward and backward field generation can occur. Eqs. (14) are then integrated using a modified beam propagation method based on the split-step algorithm [4–9,28].

4. Results and discussion

In Fig. 2 we depict the generated field at frequency ω. The figure shows that pulses are generated in both the forward and backward directions. The inset depicts the field distribution

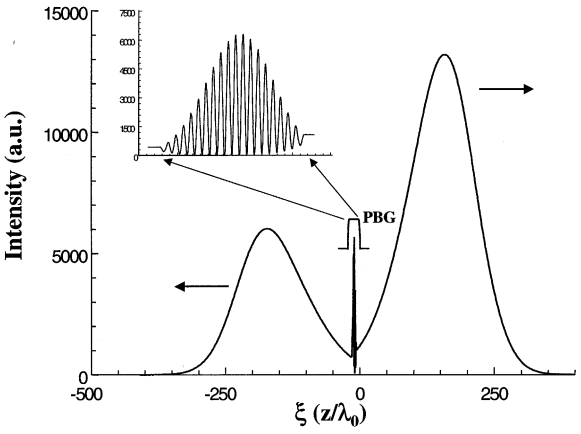

Fig. 2. Snapshot of the generated field at $\lambda = 3$ μm in both forward and backward directions. The field leaves the structure as the incident pulses exit to the right, and the interaction comes to an end. Inset: field intensity profile inside the structure at the instant the peaks of the incident pulses reach the structure.

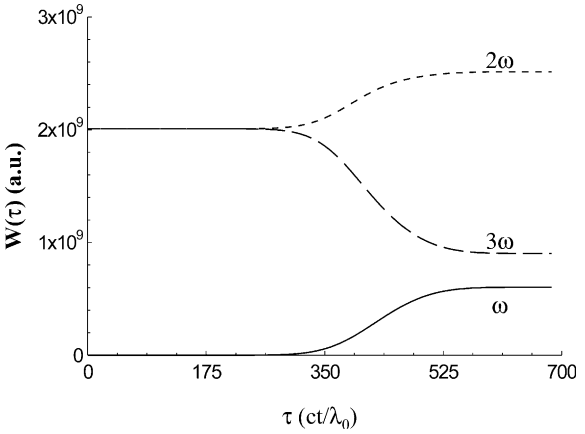

Fig. 3. Electromagnetic energy as function of time for all the three fields. We note: (a) depletion of the third harmonic frequency (– – –); (b) amplification of the second harmonic frequency (- - -); and (c) generation of the fundamental signal (—).

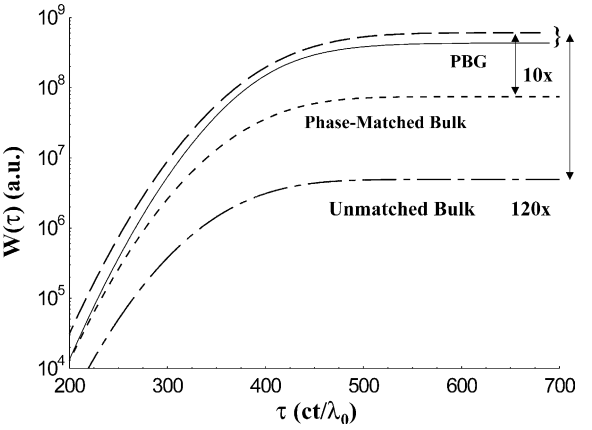

Fig. 4. Electromagnetic energy as function of time for the fields generated from the PBG structure depicted in Fig. 1 (—), and an exactly phase-matched bulk of the same length (- - -) with a refractive index $n = 1.475$. We observe that the conversion efficiency is enhanced by approximately one order of magnitude. We also show the energy attainable with the same length of unprocessed, unmatched bulk material, i.e., the refractive indices for the fields are those specified for the high index layers of Fig. 1 (lower curve (– - – -)). The higher dashed curve represents the energy output by tuning the fields to the $(3N-3)$, $(2N-2)$ and $(N-1)$ resonances. In this case, an unusual set of circumstances, i.e., simultaneously phase matched fundamental-second harmonic interaction, and three-wave mixing process, cause slightly better conversion efficiency, even if the density of modes is smaller for the pump fields as depicted in Fig. 1. In both cases the PBG performs approximately 100 times better compared to the unmatched bulk.

inside the structure at the instant the peak of the incident pulses has reached the center of the structure, and it strongly resembles the linear field profile calculated at the same frequency using the matrix transfer method in the linear case. This follows from the fact that we are dealing with deep gratings, where index discontinuities can be of order unity. As a result, no noticeable band shifts occur [23]. In Fig. 3 we plot the total energy as a function of time for all the fields, as the incident pulses traverses the structure. We define the total energy as:

$$W_j(\tau) = \frac{1}{4\pi}\int_{-\infty}^{\infty} n_j^2(\xi)|E_j(\xi,\tau)|^2\,\mathrm{d}\xi. \tag{15}$$

We note that both the fundamental and second harmonic fields experience gain at the expense of the third harmonic signal; that the third harmonic pump pulse becomes significantly depleted during a single pump pass; and that the total energy remains conserved. We stress the fact that with a $\chi^{(2)}$ of 100 pm/V and input pump field intensities of order of 100 MW/cm^2 we are able to reach the pump depletion regime with a structure approximately 10 μm (for $\lambda_0 = 1$ μm) in length. Increasing structure length can further decrease pump thresholds thanks to a corresponding increase of the density of modes for each of the pump fields.

In Fig. 4 we compare the energy output of our structure with the energy output from a structure with the same length of exactly phase matched, dispersionless bulk medium. We also compare with the energy output of an unmatched bulk material of the same length, and whose refractive indices at ω_1, ω_2 and ω_3 are taken to be $n(\omega_1) = 1.4285714$, $n(\omega_2) = 1.475$, $n(\omega_3) = 1.502$, i.e., no phase-matching conditions of any kind are introduced. The conversion efficiency obtained with the 20-period structure is approximately two orders of magnitude larger compared to the conversion efficiency of the unmatched bulk, and approximately 10 times better than the conversion efficiency of a phase-matched bulk medium whose index of refraction is chosen to be $n = 1.475$ at all frequencies. These results are obtained using incident pulses whose duration in approximately 160

optical cycles, which corresponds to approximately 1 ps. Our calculations also show that the conversion efficiency drops significantly if the phase-matching condition shown in Fig. 1 is not satisfied. The amount of dispersion we introduced in our sample in order to achieve phase-matching conditions is typical of the dispersion present in ordinary semiconductor materials.

The dashed curve in Fig. 4 is calculated using slightly different pump tuning conditions that result in another possible phase matching scheme, and highlights the flexibility of the system. Referring to Fig. 1, tuning the third and second harmonic fields to the $(3N-3)$ and $(2N-2)$ resonances causes the phase-matching condition for generation at the fundamental frequency to shift to the $(N-1)$ resonance. The figure suggests that while the density of modes is smaller for both pump fields, the conversion efficiency increases due to the following, highly unusual set of circumstances: the conditions are right for a double phase matched interaction. The first is between the fundamental and second harmonic fields, while the second is satisfied for all the fields. Clearly, these conditions take on a special meaning for up-conversion processes; simultaneous phase matched second and third harmonic generation in particular. These conditions were first discussed by Akhmanov [29], for three-wave mixing in a phase-matched bulk material. However, the prospects of phase-matching conditions for a TWM process remain to our knowledge impossible to achieve in bulk materials. Therefore, the ability to use the geometrical dispersion of the structure to compensate for material dispersion has essentially solved a long-standing problem, and thus deserves to be discussed separately.

5. Conclusions

To summarize, we have shown a new method to achieve efficient nonlinear infrared parametric generation in 1-D PBG structures. We predict conversion efficiencies well in excess of two orders of magnitude compared to bulk materials of the same length, and approximately one order of magnitude compared to an exactly phase-matched bulk medium. We take advantage of the simultaneous availability of high field localization inside a multilayer stack when tuned near band edge resonances, and of exact phase-matching conditions brought about by a combination of material and geometrical dispersion. We expect a rapid increase in conversion efficiency as the number of periods is increased. The example that we have discussed shows that it should be possible to extend these considerations to both shorter and longer wavelength regimes, and to design devices that represent a new generation of cheap, efficient parametric sources for up- and down-conversion processes. Our calculations also suggests that there are very promising prospects for efficient third harmonic generation driven by a second-order nonlinear process, under exact phase-matching conditions.

Acknowledgements

M.C. and G.D. would like to thank the US Army European Research Office for financial support. We would also like to acknowledge helpful discussions with Neşet Aközbek and A.M. Zheltikov.

References

[1] E. Yablonovitch, Phys. Rev. Lett. 58 (1987) 2059.
[2] J.D. Joannopoulos, P.R. Villeneuve, Nature London 386 (1997) 143.
[3] C.M. Soukoulis, Phys. Scr. T66 (1996) 146.
[4] M. Scalora, J.P. Dowling, C.M. Bowden, M.J. Bloemer, J. Appl. Phys. 73 (1994) 1368.
[5] M. Scalora, J.P. Dowling, C.M. Bowden, M.J. Bloemer, J. Appl. Phys. 76 (1994) 2023.
[6] J.P. Dowling, M. Scalora, M.J. Bloemer, C.M. Bowden, J. Appl. Phys. 75 (1994) 1896.
[7] M. Scalora, R.J. Flynn, S.B. Reinhardt, R.L. Fork, M.D. Tocci, M.J. Bloemer, C.M. Bowden, H.S. Ledbetter, J.M. Bendickson, J.P. Dowling, R.P. Leavitt, Phys. Rev. E 54 (1996) R1078.
[8] M. Scalora, M.J. Bloemer, A.S. Pethel, J.P. Dowling, C.M. Bowden, A.S. Manka, J. Appl. Opt. 83 (1998) 2377.
[9] M. Scalora, M.J. Bloemer, A.S. Manka, J.P. Dowling, C.M. Bowden, R. Viswanathan, J.W. Haus, Phys. Rev. A 56 (1997) 3166.

[10] J.W. Haus, R. Viswanathan, M. Scalora, A.G. Kalocsai, J.D. Cole, J. Theimer, Phys. Rev. A 57 (1998) 2120.
[11] J.C. Knight, T.A. Birkes, P.St. Russel, J.P. De Sandro, J. Opt. Soc. Am. A 15 (1998) 748.
[12] W. Chen, D.L. Mills, Phys. Rev. Lett. 58 (1987) 160.
[13] J.E. Sipe, H.G. Winful, Opt. Lett. 13 (1988) 132.
[14] S. John, N. Akozbek, Phys. Rev. Lett. 71 (1993) 1168.
[15] C.M. de Sterke, D.G. Salinas, J.E. Sipe, Phys. Rev. E 54 (1996) 1969.
[16] B.J. Eggleton, R.E. Slusher, C.M. de Sterke, P.A. Krug, J.E. Sipe, Phys. Rev. Lett. 76 (1996) 160.
[17] C. Conti, S. Trillo, G. Assanto, Phys. Rev. Lett. 78 (1997) 2341.
[18] J. Martorell, R. Vilaseca, R. Corbalan, Appl. Phys. Lett. 70 (1997) 702.
[19] J. Martorell, R. Vilaseca, R. Corbalan, Phys. Rev. A 55 (1997) 4520.
[20] J. Martorell, R. Vilaseca, R. Corbalan, J. Opt. Soc. Am. B 15 (1998) 2581.
[21] C. Simonneu, J.P. Debray, J.C. Harmand, P. Vidakovic, D.J. Lovering, J.A. Levenson, Opt. Lett. 23 (1997) 1775.
[22] A.V. Balakin, D. Boucher, V.A. Bushev, N.I. Koroteev, B.I. Mantsyzov, P. Masselin, I.A. Ozheredov, A.P. Shurinov, Opt. Lett. 24 (1999) 793.
[23] M. Centini, C. Sibilia, M. Scalora, G. D'Aguanno, M. Bertolotti, M.J. Bloemer, C.M. Bowden, I. Nefedov, Phys. Rev. E 60 (1999) 4891.
[24] G. D'Aguanno, M. Centini, C. Sibilia, M. Bertolotti, M. Scalora, M.J. Bloemer, C.M. Bowden, Opt. Lett. 24 (1999) 1663.
[25] V. Balakin, V.A. Bushuev, B.I. Mantsyzov, P. Masselin, I.A. Ozheredov, A.P. Shkurinov, JETP Lett. 70 (1999) 725.
[26] M. Born, E. Wolf, Principles of Optics, 6th Edition, Pergamon Press, Oxford, 1980.
[27] J.M. Bendickson, J.P. Dowling, M. Scalora, Phys. Rev. E 53 (1996) 4107.
[28] M. Scalora, M.E. Crenshaw, Opt. Commun. 108 (1994) 191.
[29] S.A. Akhmanov, R.V. Khokhlovnce, Problemy Nelineinoi Optiki, Gordon and Breach, NY, 1972 (translated from the original Russian edition, Academy of Sciences of the USSR, 1964).